Diagnostic Performance of Multidetector Computed Tomography (MDCT) in Diagnosis of Sinus Variations

Ahmed M. Alsowey[1A], Ghada Abdulmonaem[1B], Ahmed Elsammak[1C], Yasser Fouad[2D]

[1] Department of Radiodiagnosis, Faculty of Medicine, Zagazig University, Zagazig, Egypt
[2] Department of Otorhinolaryngology, Head and Neck Surgery, Faculty of Medicine, Zagazig University, Zagazig, Egypt

Author's address: Ahmed M. Alsowey, Department of Radiodiagnosis, Faculty of Medicine, Zagazig University, Zagazig, Egypt, e-mail: ahmedalsowey@yahoo.com

Summary

Background: In this prospective study, we looked for correlations between anatomic variants of paranasal sinuses and chronic or recurrent sinusitis.

Material/Methods: Two hundred and forty (240) patients with clinical features of chronic rhinosinusitis were examined; patients with first-onset or allergic sinusitis and pregnant females were excluded. Routine multi-slice CT of the paranasal sinuses was performed to look for mucosal disease of the paranasal sinuses, drainage pathways, and presence of anatomical variations and their relation to known sinus drainage pathways.

Results: Anatomic variations were very frequent, and we classified them into four easily recognized groups: nasal septum variations, middle turbinate variations, uncinate process variations, and ethmoidal variations. Deviated nasal septum was the most frequent variation in patients with chronic or recurrent sinusitis, and it was detected in 48.8% of cases. Agger nasi cells and concha bullosa were equally frequent (30.6%), and Haller cells were detected in 11.2%. Uncinate process variations were detected in 18.1%, and the large ethmoid bulla was detected in 10%.

Conclusions: The importance of anatomic variations is that they can compromise drainage pathway of the related sinus, which results in inflammatory sinus disease. Anatomical variations are not diseases on their own and may be present as incidental findings in patient with chronic sinusitis.

MeSH Keywords: Endoscopy • Multidetector Computed Tomography • Paranasal Sinuses

PDF file: http://www.polradiol.com/abstract/index/idArt/903684

Background

Chronic rhinosinusitis is a common condition in which the paranasal sinuses (PNS) become inflamed and swollen for at least eight weeks despite treatment attempts [1]. It is also known that chronic rhinosinusitis interferes with drainage and causes mucus to build up. It is one of the most common illnesses of our times, and it is increasing in epidemic proportions throughout the world [2]. Chronic or recurrent sinusitis has been known to negatively impact health-related quality of life [3].

In recent years, functional endoscopic sinus surgery (FESS) has become a gold standard in the treatment of chronic rhinosinusitis. Treatment outcomes depend on the preoperative assessment and qualification of patients. Multi-slice computed tomography (MSCT) of the paranasal sinuses exhibits good sensitivity and specificity for the diagnosis of chronic rhinosinusitis. In combination with medical history and physical findings, MSCT may increase accuracy of diagnosing chronic rhinosinusitis [4]. With the advent of FESS and coronal MSCT, considerable attention has been directed towards the anatomy of the paranasal region. Detailed knowledge of anatomic variations in the paranasal sinus region is critical for surgeons performing endoscopic sinus surgery as well as for radiologists involved in the preoperative work-up. MSCT, especially in the coronal plane, is the most common method used by surgeons due to its similarity to the surgical orientation [2].

MSCT plays a central role in the modern management of chronic rhinosinusitis due to its ability to demonstrate the

primary obstructive pathology, to delineate mucosal disease, and to image distal structures that cannot be viewed with direct endoscopy, such as the posterior ethmoid sinus [2].

The reported frequency of anatomic variations in patients with chronic rhinosinusitis is as follows: agger nasi cells in 15%, Haller cells in 7%, conchae bullosa in 30%, paradoxical middle turbinate in 24%, and septal deviation in 21% of patients [5]. Outcomes of FESS for chronic rhinosinusitis depend on an accurate evaluation of the disease and paranasal anatomic variations. After identification of these variations, FESS, with usually minimal invasive operations, can provide dramatic relief of chronic or recurrent symptoms of sinusitis [4].

Anatomic variations of the paranasal sinuses compromise already narrow drainage pathways and produce significant obstruction; by themselves, they do not represent disease states. Such anatomic variants occur frequently, have a potential impact on surgical safety, and need to be specifically sought in the preoperative evaluation [2].

MSCT with its capability of displaying bone and soft tissues is the current diagnostic modality of choice for evaluating the ostiomeatal complex. MSCT is used both as a diagnostic tool to identify anatomical anomalies and mucosal pathology and as a preoperative map to guide the surgeon through the challengingly convoluted and variable anatomy of the area [2,3].

The aim of this study is to investigate anatomical variations diagnosed on coronal MDCT of the paranasal sinuses in patients who underwent endoscopic sinus surgery and to investigate whether these variations were actively involved in the etiology of sinusitis.

Material and Methods

Patients

This study included 240 patients referred from the ENT Department, Zagazig University Hospital, for routine MSCT of the paranasal sinuses during the period from May 2014 to October 2016. All patients who had symptoms of chronic rhinosinusitis refractory to medical therapy and would be candidates for endoscopic sinus surgery were included in the study. Patients with first-onset or allergic sinusitis and pregnant females were excluded. The protocol and informed consent forms used in this study were approved by the Institutional Review Board (IRB) of Zagazig University. All participants signed a written informed consent and filled a written survey including demographic and clinical data. In all the included patients, we gathered data regarding complete history of symptoms suggestive of chronic rhinosinusitis and findings of ENT examination, MSCT examination of the paranasal sinuses (PNS), and diagnostic endoscopy.

Methods

MSCT examination

Parameters

MSCT was performed using 128-row multi-slice CT scanner (PHILIPS ingenuity 128-slice CT scanner). Both direct coronal and axial scanning was performed. The coronal scans extended from the anterior wall of the frontal sinus to the posterior wall of the sphenoid sinus. In the axial scans, the beam was parallel to the hard palate, and the scans extended from the hard palate to the top of the frontal sinus. Slice thickness was 4 mm, and the table incrimination was 3 mm. We used 130 KV and 150 mA/sec. Scan time was 1.5 sec. Window widths were about 1300: 2000 and window levels about –80: –200. Both soft tissue and bone windows were obtained. No intravenous contrast was used. A high-resolution algorithm was used for enhancement of the fine bony details of the ostiomeatal complex.

Image interpretation

Films were inspected in a routine, standardized fashion to insure that small details were not missed using PACS (picture archiving and communicating system). The main items reviewed were as follows: paranasal sinus groups, drainage pathways, lateral nasal wall, nasal septum and surrounding structures. The presence of anatomical variations that either compromised the sinus drainage pathways or not was assessed.

To assess the severity of chronic rhinosinusitis, the disease was scored according to the criteria of Lund-Mackay score[(5)]. Full opacification, semi-opacification, and normal mucosa were scored as 2, 1, and 0, respectively. Open ostiomeatal complex (OMC) was scored as 0, and as 2 when closed. Some anatomical variations and their effects on the severity of sinus disease (sinuses with close relation or neighboring the analyzed anatomical variation) were compared statistically (e.g., rate of concha bullosa and the severity of maxillary sinus disease).

Endoscopic evaluation

Intraoperative endoscopic evaluation

Endoscopic sinus surgery was performed in all patients. The surgery aimed to ventilate all the affected sinuses according to the preoperative CT. During surgery, all affected sinuses were opened and ventilated, and the surgeon commented on the mucosal state of each sinus. Also during surgery, all the anatomical variations were reported, whether surgical correction of these variations was performed or not.

Endoscopic interpretation

Non-affected sinuses were defined by the presence of apparent normal-colored mucosa with absence of polyps or inspissated mucopurulent discharge. Unhealthy or affected sinuses had one of these criteria.

Table 1. MDCT – affected sinuses in 240 patients with chronic rhinosinusitis.

The affected sinus	Unilateral, N (%)			Bilateral, N (%)	Total, N (%)
	Right, N (%)	Left, N (%)	Total, N (%)		
Maxillary	44 (18.3%)	63 (26.3%)	107 (44.6%)	88 (36.7%)	195 (81.3%)
Anterior ethmoid	36 (15%)	23 (9.6%)	59 (24.6%)	26 (10.8%)	85 (35.4%)
Frontal	23 (9.6%)	21 (8.8%)	44 (18.3%)	48 (20%)	92 (38.3%)
Posterior ethmoid	18 (7.5%)	20 (8.3%)	38 (15.8%)	36 (15%)	74 (30.8%)
Sphenoid	31 (12.9%)	40 (16.7%)	71 (29.6%)	45 (18.8%)	116 (48.3%)

The anatomical variations that were assessed on endoscopy included nasal septal variations (deviation, spur), ethmoidal cell variations (hypertrophied ethmoid bulla, large agger nasi cells obstructing frontal sinus drainage, Haller cells, Onodi cells), middle turbinate variations (large MT, paradoxical MT), and uncinate process variations (flattened, medially bent, hypertrophied, atelectasis). We differentiated mild and severe nasal septal deviations and mild and severe concha bullosa according to the surgeon decision, as the cases necessitating surgical correction were defined as severe.

Statistical analysis

Qualitative data were expressed as absolute frequencies (count) and relative frequencies (percentage). The McNemar test was used for paired categorical data. Interrater agreement in detection of anomalies between MDCT and endoscopy was analyzed using the McNemar test and the kappa (K) statistic. Agreement was reached, if the p value of the McNemar test was insignificant and the p value of the kappa statistic was significant. Criteria for the strength of agreement were as follows: K <0.2, poor; K 0.21–0.40, fair; K 0.41–0.60, moderate; K 0.61–0.80, good; and K 0.81–1.00, very good. Validity of the MDCT-based assessment of the nose and sinuses was calculated on the basis of 2×2 contingency tables with endoscopic findings as the reference standard. Sensitivity, specificity, positive predictive values, negative predictive values, and accuracy with 95% confidence intervals were calculated. All tests were two-tailed and p <0.05 was considered significant. All statistics were calculated using SPSS 22.0 for Windows (SPSS Inc., Chicago, IL, USA) and MedCalc 13 for Windows (MedCalc Software bvba, Ostend, Belgium).

Results

This study included 240 patients with chronic rhinosinusitis (138 (57.5%) males, 102 (42.5%) females). Their ages ranged from 20 to 61 years, with the mean age of 40.5 years.

The most common clinical presentations were headache (52.5%), runny nose (35%), postnasal discharge (33.8%), and nasal obstruction (25%).

Many anatomic variants were detected in this study that could be incidental or causative of the sinonasal inflammatory disease. These anatomic variants were reported on both sides, except for the nasal septum which is a single structure (Table 1).

All patients had the diagnosis of chronic rhinosinusitis and were operated on for that reason; thus, all patients had evidence of mucosal disease in at least one of the paranasal sinuses. The distribution of the affected sinuses in the study group on both CT study and intraoperative endoscopy is shown in Table 2. Statistical comparison between the total number of positive findings on CT and endoscopy in each sinus was performed (Table 2).

Anatomical variants were classified into four easily recognizable groups; Group I: Nasal septum variations; Group II: Ethmoidal variations; Group III: Middle turbinate variations; Group IV: Uncinate process variations. Because some patients had more than one affected sinus on MSCT, the total number of affected sinuses exceeds the number of patients.

The ethmoidal anatomical variations in the examined patients included hypertrophied ethmoidal bulla, large agger nasi cells, Haller's cells, and Onodi cells.

The anatomic variants of the middle turbinate in the examined patients included pneumatized middle turbinate (concha bullosa) that may or may not compromise the ostiomeatal complex (OMC), which might necessitate surgery, and paradoxical middle turbinate.

Different anatomic variations of the uncinate process detected in our study revealed lateral deviation, medial deviation, pneumatization, hypertrophy, and atelectatic uncinate process (Table 3).

We found very good agreement between MDCT and endoscopy in diagnosing nasal septum variations, with k=0.665, p≤0.001, standard error=0.048. There was very good agreement between MDCT and endoscopy in diagnosing nasal spur variations, with k=0.828, p≤0.001, standard error=0.026. There was moderate agreement between MDCT and endoscopy in diagnosing ethmoidal variations, with k=0.743, p≤0.001, standard error=0.031. There was moderate agreement between MDCT and endoscopy in diagnosing hypertrophic ethmoid bulla, with k=0.755, p value≤0.001, standard error=0.030. There was very good agreement between MDCT and endoscopy in diagnosing agger nasi cells, with k=0.866, p≤0.001, standard error=0.023. There was moderate agreement between

Table 2. Comparison between MDCT and endoscopy in the assessment of 240 patients (480 sides).

Findings	MDCT		Endoscope		p-Value*
	No.	%	No.	%	
Nasal septum variations	(N=240)		(N=240)		
Absent	102	42.5%	116	48.3%	0.040
Present	138	57.5%	124	51.7%	
Nasal spur variation	(N=480)		(N=480)		
Absent	180	37.5%	187	39%	0.337
Present	300	62.5%	293	61%	
Ethmoidal variations	(N=480)		(N=480)		
Absent	175	36.5%	174	36.3%	1.000
Present	305	63.5%	306	63.8%	
Hypertrophic ethmoid bulla	(N=480)		(N=480)		
Absent	210	43.8%	181	37.7%	<0.001
Present	270	56.3%	299	62.3%	
Large agger nasi cell	(N=480)		(N=480)		
Absent	189	39.4%	196	40.8%	0.281
Present	291	60.6%	284	59.2%	
Haller's cell	(N=480)		(N=480)		
Absent	186	38.8%	199	41.5%	0.131
Present	294	61.3%	281	58.5%	
Onodi cell	(N=480)		(N=480)		
Absent	212	44.2%	214	44.6%	0.883
Present	268	55.8%	266	55.4%	
Middle turbinate variations	(N=480)		(N=480)		
Absent	202	42.1%	202	42.1%	0.838
Present	278	57.9%	278	57.9%	
Uncinate process variation	(N=480)		(N=480)		
Absent	186	38.8%	191	39.8%	0.551
Present	294	61.3%	289	60.2%	
Maxillary sinus affection	(N=480)		(N=480)		
Absent	174	36.3%	167	34.8%	0.360
Present	306	63.8%	313	65.2%	
Anterior ethmoidal affection	(N=480)		(N=480)		
Absent	218	45.4%	219	45.6%	1.000
Present	262	54.6%	261	54.4%	
Frontal affection	(N=480)		(N=480)		
Absent	202	42.1%	213	44.4%	0.082
Present	278	57.9%	267	55.6%	
Posterior ethmoidal affection	(N=480)		(N=480)		
Absent	189	39.4%	190	39.6%	1.000
Present	291	60.6%	290	60.4%	
Sphenoidal affection	(N=480)		(N=480)		
Absent	205	42.7%	192	40%	0.037
Present	275	57.3%	288	60%	

Qualitative data are expressed as counts and percentages (%); * McNemar's test; p<0.05 is significant.

Table 3. Concordance between MDCT and endoscopy in the assessment of 240 patients (480 sides).

Findings	Concordant	+ve/+ve	−ve/−ve	Discordant	−ve/+ve	+ve/−ve
Nasal septum variations	200 (83.3%)	111 (46.3%)	89 (37.1%)	40 (16.7%)	13 (5.4%)	27 (11.3%)
Nasal spur variation	441 (91.9%)	277 (57.7%)	164 (34.2%)	39 (8.1%)	16 (3.3%)	23 (4.8%)
Ethmoidal variations	423 (88.1%)	277 (57.7%)	146 (30.4%)	57 (11.9%)	29 (6%)	28 (5.8%)
Hypertrophic ethmoid bulla	423 (88.1%)	256 (53.3%)	167 (34.8%)	57 (11.9%)	43 (9%)	14 (2.9%)
Large agger nasi cell	449 (93.5%)	272 (56.7%)	177 (36.9%)	31 (6.5%)	12 (2.5%)	19 (4%)
Haller's cell	417 (86.9%)	256 (53.3%)	161 (33.5%)	63 (13.1%)	25 (5.2%)	38 (7.9%)
Onodi cell	434 (90.4%)	244 (50.8%)	190 (39.6%)	46 (9.6%)	22 (4.6%)	24 (5%)
Middle turbinate variations	456 (95%)	266 (55.4%)	190 (39.6%)	24 (5%)	12 (2.5%)	12 (2.5%)
Uncinate process variation	435 (90.6%)	269 (56%)	166 (34.6%)	45 (9.4%)	20 (4.2%)	25 (5.2%)
Maxillary sinus affection	437 (91%)	288 (60%)	149 (31%)	43 (9%)	25 (5.2%)	18 (3.8%)
Anterior ethmoidal affection	445 (92.7%)	244 (50.8%)	201 (41.9%)	35 (7.3%)	17 (3.5%)	18 (3.8%)
Frontal affection	447 (93.1%)	256 (53.3%)	191 (39.8%)	33 (6.9%)	11 (2.3%)	22 (4.6%)
Posterior ethmoidal affection	437 (91%)	269 (56%)	168 (35%)	43 (9%)	21 (4.4%)	22 (4.6%)
Sphenoidal affection	447 (93.1%)	265 (55.2%)	182 (37.9%)	33 (6.9%)	23 (4.8%)	10 (2.1%)

Qualitative data are expressed as counts and percentages (%); Nominator – MDCT; Dominator – Endoscope.

Table 4. Agreement between MDCT and endoscopy in the assessment of 240 patients (480 sides).

Findings	p-Value[#]	Kappa	SE	95%CI	p-Value*
Nasal septum variations	0.040	0.665	0.048	0.571–0.759	<0.001
Nasal spur variation	0.337	0.828	0.026	0.776–0.880	<0.001
Ethmoidal variations	1.000	0.743	0.031	0.681–0.806	<0.001
Hypertrophic ethmoid bulla	<0.001	0.755	0.030	0.696–0.814	<0.001
Large agger nasi cell	0.281	0.866	0.023	0.820–0.911	<0.001
Haller's cell	0.131	0.727	0.032	0.664–0.790	<0.001
Onodi cell	0.883	0.806	0.027	0.753–0.859	<0.001
Middle turbinate variations	0.838	0.897	0.020	0.857–0.937	<0.001
Uncinate process variation	0.551	0.803	0.027	0.749–0.858	<0.001
Maxillary sinus affection	0.360	0.804	0.028	0.749–0.860	<0.001
Anterior ethmoidal affection	1.000	0.853	0.023	0.806–0.900	<0.001
Frontal affection	0.082	0.860	0.023	0.814–0.906	<0.001
Posterior ethmoidal affection	1.000	0.813	0.027	0.759–0.866	<0.001
Sphenoidal affection	0.037	0.858	0.024	0.812–0.905	<0.001

[#] McNemar's test; SE – Standard Error; 95%, CI – 95% confidence interval; * p value of kappa statistics; p<0.05 is significant.

MDCT and endoscopy in diagnosing Haller's cells, with k=0.727, p≤0.001, standard error=0.032. There was very good agreement between MDCT and endoscopy in diagnosing Onodi cells, with k=0.806, p≤0.001, standard error=0.027. There was very good agreement between MDCT and endoscopy in diagnosing middle turbinate variations, with k=0.897, p≤0.001, standard error=0.020. There was very good agreement between MDCT and endoscopy in diagnosing uncinate process variations, with k=0.803, p≤0.001, standard error=0.027. There was very good agreement between MDCT and endoscopy in diagnosing maxillary sinus affection, with k=0.804, p≤0.001,

Table 5. Sensitivity, specificity, positive and negative predictive values, and accuracy of MDCT in the assessment of 240 patients (480 sides).

Findings	SN	SP	Acc	PPV	NPV
Nasal septum variations	89.5%	76.7%	83.3%	80.4%	87.3%
Nasal spur variation	94.5%	87.7%	91.9%	92.3%	91.1%
Ethmoidal variations	90.5%	83.9%	88.1%	90.8%	83.4%
Hypertrophic ethmoid bulla	85.6%	92.3%	88.1%	94.8%	79.5%
Large agger nasi cell	95.8%	90.3%	93.5%	93.5%	93.7%
Haller's cell	91.1%	80.9%	86.9%	87.1%	86.6%
Onodi cell	91.7%	88.8%	90.4%	91.0%	89.6%
Middle turbinate variations	95.7%	94.1%	95.0%	95.7%	94.1%
Uncinate process variation	93.1%	86.9%	90.6%	91.5%	89.2%
Maxillary sinus affection	92.0%	89.2%	91.0%	94.1%	85.6%
Anterior ethmoidal affection	93.5%	91.8%	92.7%	93.1%	92.2%
Frontal affection	95.9%	89.7%	93.1%	92.1%	94.6%
Posterior ethmoidal affection	92.8%	88.4%	91.0%	92.4%	88.9%
Sphenoidal affection	92.0%	94.8%	93.1%	96.4%	88.8%

SN – sensitivity; SP – specificity; Acc – accuracy; PPV – positive predictive value; NPV – negative predictive value.

standard error=0.028. There was very good agreement between MDCT and endoscopy in diagnosing anterior ethmoidal sinus affection, with k=0.853, p≤0.001, standard error=0.023. There was very good agreement between MDCT and endoscopy in diagnosing frontal sinus affection, with k=0.860, p≤0.001, standard error=0.023. There was very good agreement between MDCT and endoscopy in diagnosing posterior ethmoidal sinus affection, with k=0.813, p=<0.001, standard error=0.027. There was very good agreement between MDCT and endoscope in diagnosing sphenoidal sinus affection, with k=0.858, p≤0.001, standard error=0.024 (Table 4).

The values of sensitivity, specificity, PPV, NPV, and accuracy for MDCT and endoscopy are shown in Table 5.

Discussion

Chronic or recurrent rhinosinusitis is one of the most common illnesses of our times, and it is increasing in epidemic proportions throughout the world [6].

In chronic or recurrent paranasal sinus disease, MSCT is used both as a diagnostic tool to identify anatomical anomalies and mucosal pathology and as a preoperative map to guide the surgeon prior to endoscopic sinus surgery. Ostiomeatal complex is the key area in the pathogenesis of chronic or recurrent sinusitis; many anatomic variations may affect this region and may play an important role in the obstruction of the ostiomeatal complex [5]. One of the prerequisites for successful FESS is knowledge of the complex anatomy of paranasal sinuses. The anatomy of the paranasal sinuses is variable, and it is important to appreciate the clinical and surgical significance of these anatomic variations [7].

It is important to properly prepare patients for MDCT in order to eliminate as many reversible diseases as possible, thus eliminating any acute sinusitis components. This, in turn, allows for an optimal delineation of chronic, nonreversible disease components [8].

In our study, high-resolution imaging was performed, which improved spatial resolution with enhancement of the fine bony details of the ostiomeatal region.

MDCT is helpful in evaluating the ostiomeatal complex, soft tissue details and their relationship to bone and air containing sinuses. Coronal scans can detect the site and type of inflammation, and they optimally show the ostiomeatal unit, the relationship between the brain and the ethmoid roof, and the relationship between the orbits and the paranasal sinuses. Moreover, coronal images correlate with the surgical approach in FESS [5]. This is in accordance with Dalgorf and Harvey [8] who found that coronal MDCT is now the study of choice for chronic sinusitis, since it simulates the endoscopic view of the sinonasal cavity and provides a bony road map for surgery. In the remaining cases, in addition to the coronal plane, axial scans were obtained, as they show in an excellent way the paranasal sinuses, the pterygopalatine fossa, and especially the relationship between the optic nerve and the posterior ethmoid and sphenoid sinuses [9].

Azila et al. 2011 [10] propose that stenosis of the ostiomeatal complex, resulting from either anatomical variations or hypertrophied mucosa, can cause obstruction and stagnation of secretions that may then become infected. They stated that, when the obstructed drainage pathway reopens, reversal of the inflammatory process will result.
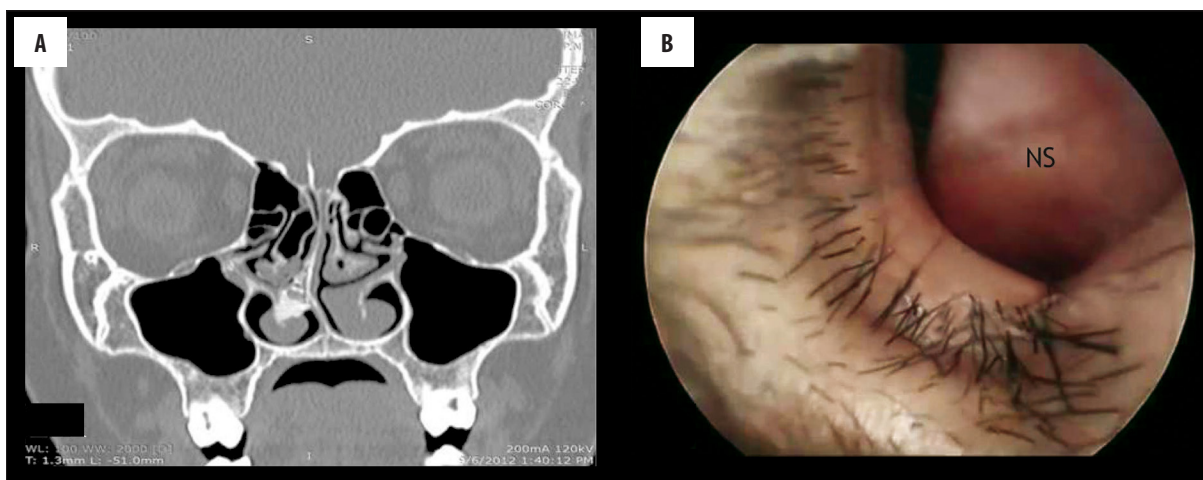
Figure 1. (**A**) MSCT, coronal scans of PNS show right-sided deviation of the bony nasal septum with a bony nasal septal spur on the right that is associated with bilateral concha bullosa, larger on the right. (**B**) Endoscopic image revealed the same findings of right bony nasal septal spur (NS).
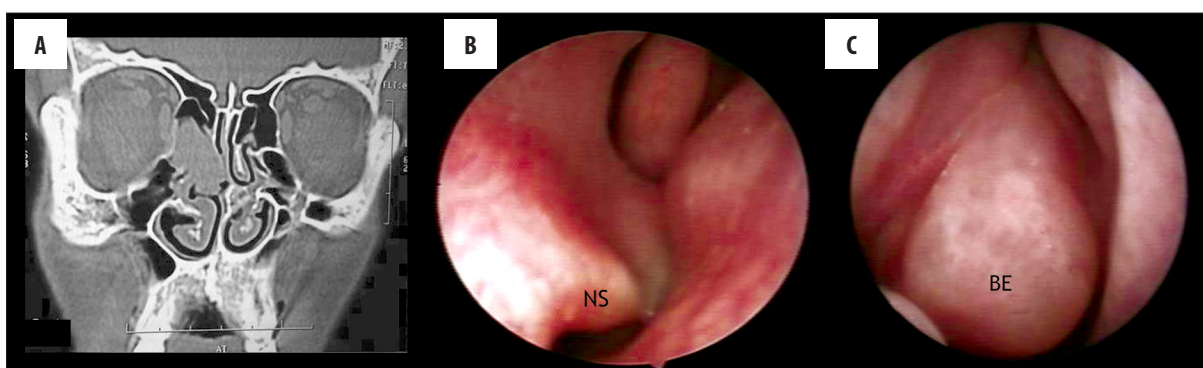

Figure 2. (**A**) MSCT, coronal scans of PNS show left-sided deviation of bony nasal septum associated with left-sided bony nasal septum spur; additionally, right-sided huge bulla ethmoidalis can be observed. (**B, C**) endoscopic images revealed the same findings of left-sided bony nasal septum spur (NS) and huge bulla ethmoidalis (BE).

Nasal septal variations were the most common variations detected in patients with inflammatory sinus disease; in 72.5% of patients. Septal deviation is the most common septal variation; when severe enough, the deviated septum may compress the middle turbinate bone laterally, narrowing the middle meatus and causing obstruction. In our study, nasal septum deviation obstructed the middle meatus in 12.5% of cases [11]. The reported prevalence of septal variations in the literature ranges between 40% and 96.9% due to varying morphological features and the extent of deviation. Luo et al. 2012 [11], who defined deviation as crooked nasal septum impinging on the adjacent structures, reported a prevalence of 40%. Other, less important septal variations include pneumatized nasal septum and nasal spur (Figures 1, 2).

Middle turbinate variations were frequent in our study and were detected in 48.1% of the examined sides. Concha bullosa was the most frequent variation of the middle turbinate (30.6%). It is defined as pneumatization of the middle turbinate due to extension of adjacent ethmoidal air cells; the reported prevalence of concha bullosa ranges from 40% to 80%, and the highest prevalence is seen in patients with chronic sinusitis [12].

Katyaet al. 2015 [2] reported that concha bullosa can, when sufficiently large, produce signs and symptoms by encroaching upon the infundibulum. In our study, concha bullosa was compromising the infundibulum in 9.4% of the examined sinuses. Paradoxical middle turbinate is less common, and it was detected in 10% of the examined sinuses. Kaygusuz et al. 2014 [9] reported a prevalence of 7.9%. The normal convexity of the middle turbinate bone is directed medially towards the nasal septum, when paradoxically curved, the convexity is directed laterally towards the lateral nasal wall. When it is large enough, it obstructs drainage pathways. Septal deviation was associated with paradoxical middle turbinate in 84% of cases.

Ethmoidal variations were common in this study, and they were detected in 51% of the examined sides. Agger nasi cells, the most constant ethmoidal air cells, were defined by Alkire and Bhattacharyya in 2010 [13] as extensions of the anterior ethmoidal air cells below the frontal sinus and inferolaterally to the lacrimal sinus. They are located anteriorly and superiorly to the insertion of the middle turbinate bone along the lateral nasal wall. Their reported prevalence ranges from 10% to 89%. In our study, agger nasi cells were detected in 30.6% of the examined sides. The importance of agger nasi cells is that they can
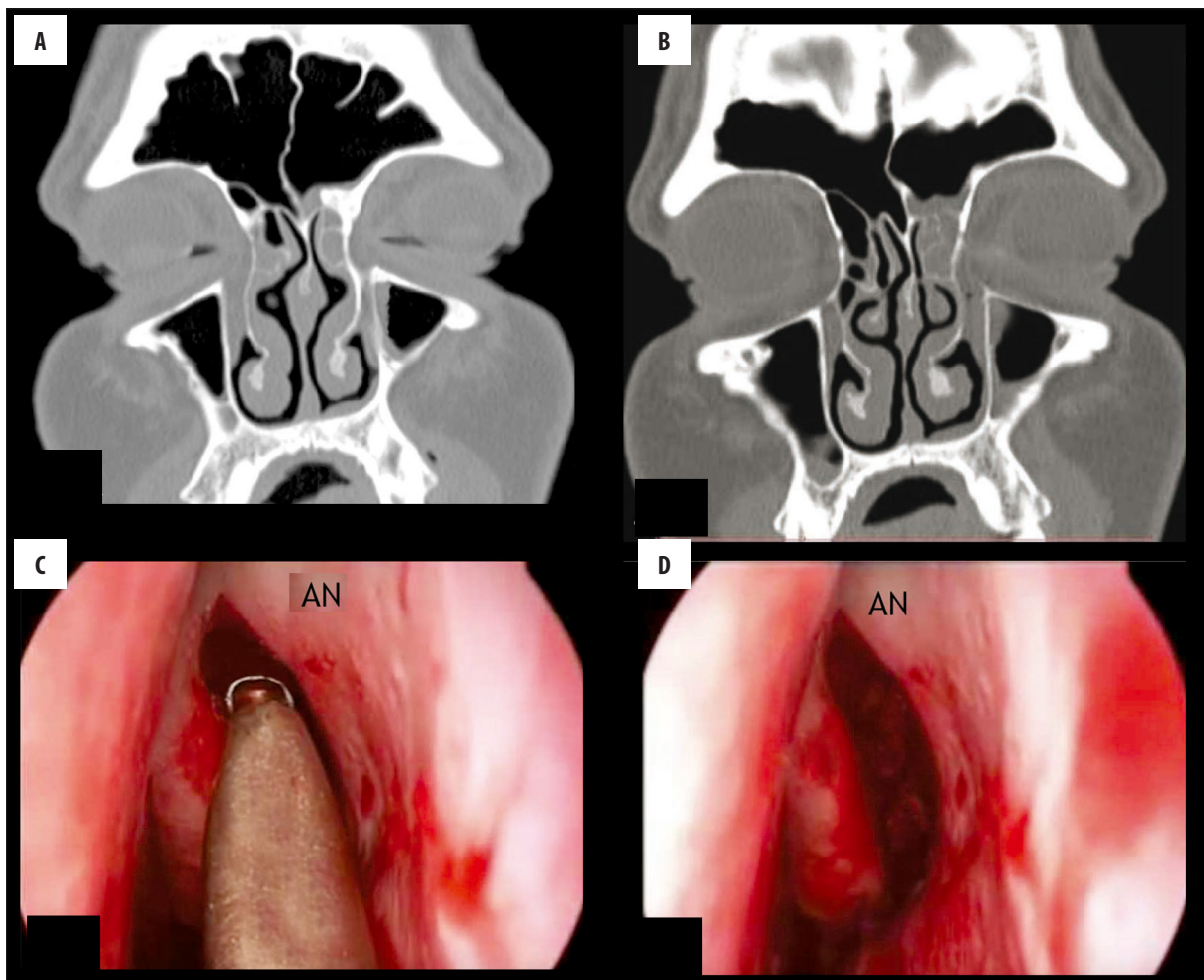
Figure 3. (**A, B**) MSCT, coronal scans of PNS show bilateral agger nasi cells, obliterated on the left side, with ipsilateral moderate and mild ethmoidal and maxillary mucosal thickening, respectively. (**C, D**) Endoscopic images revealed left-sided (LT) agger nasi (AN) cells.
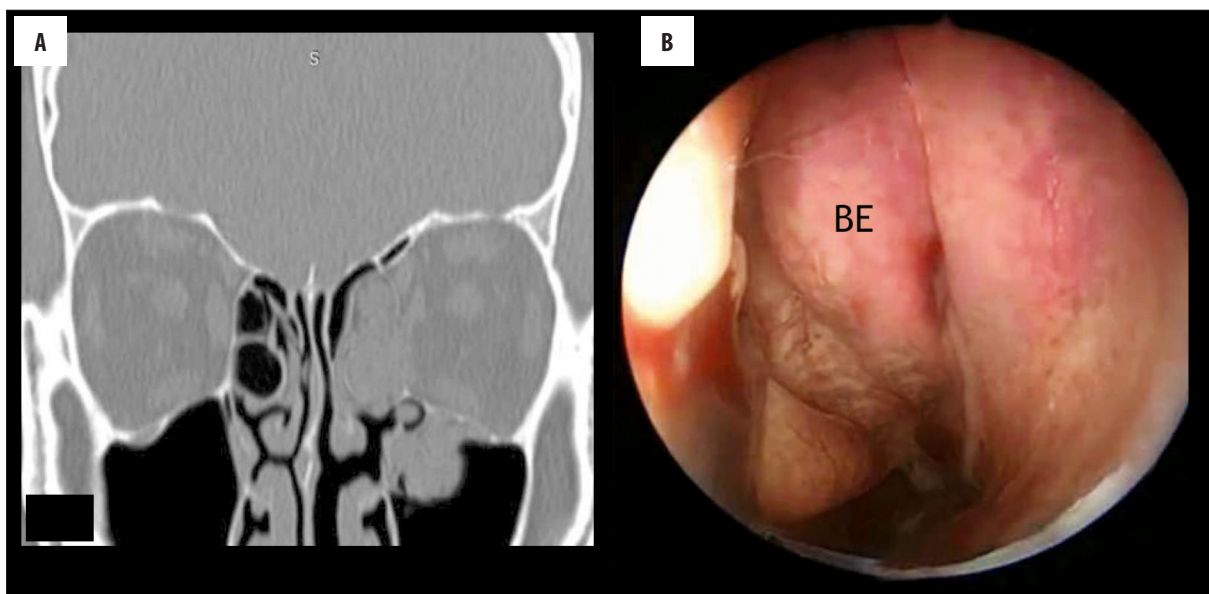

Figure 4. (**A**) MSCT, coronal scan of PNS shows left-sided, opacified, huge bulla ethmoidalis associated with left maxillary sinusitis. (**B**) Endoscopic image revealed the same findings of left-sided, enlarged bulla (BE).
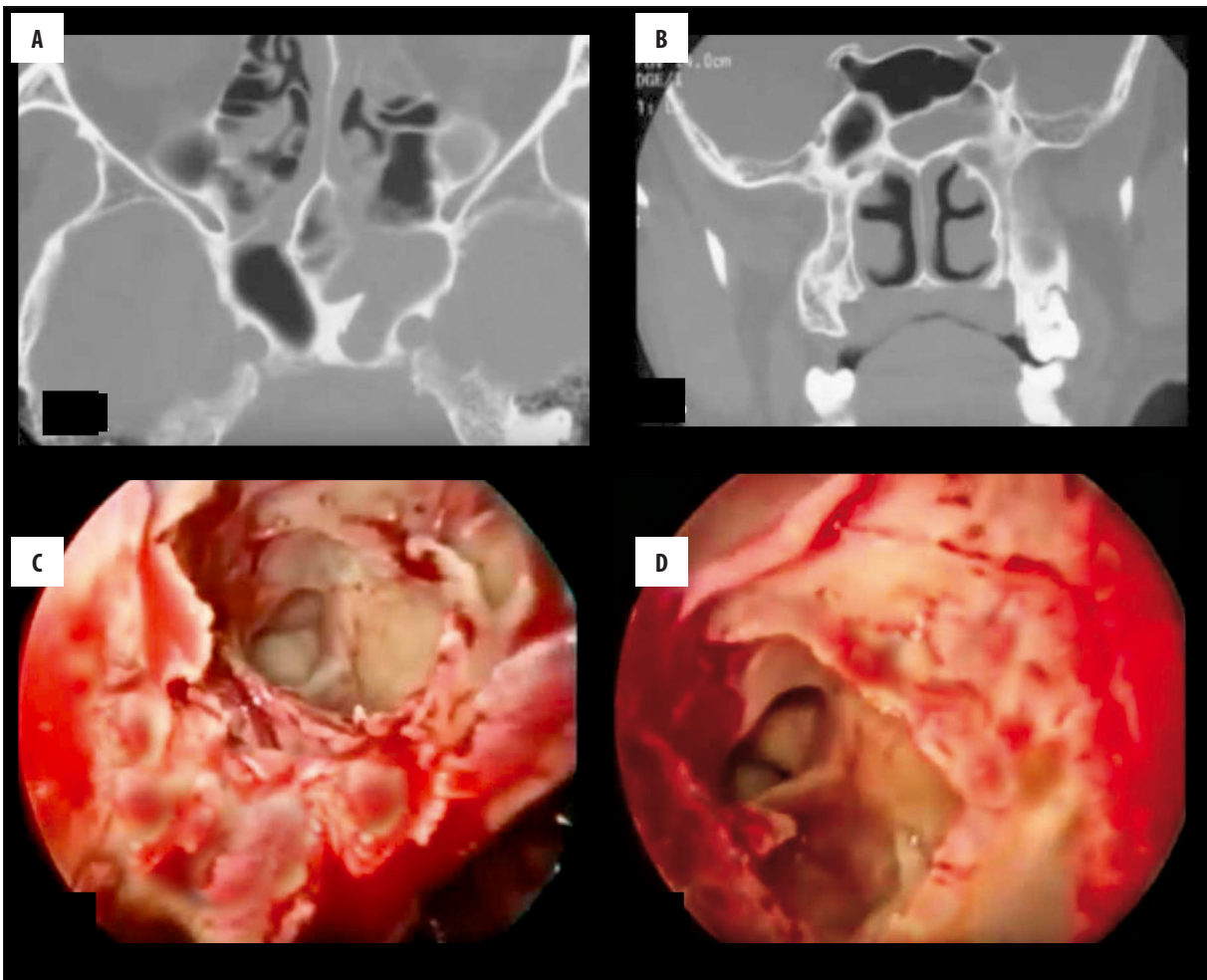
Figure 5. (**A, B**) MSCT, axial and coronal scans of PNS reveal Onodi cell within the left ethmoidal air cells, associated with left sphenoidal sinusitis. (**C, D**) Endoscopic images revealed the same findings.
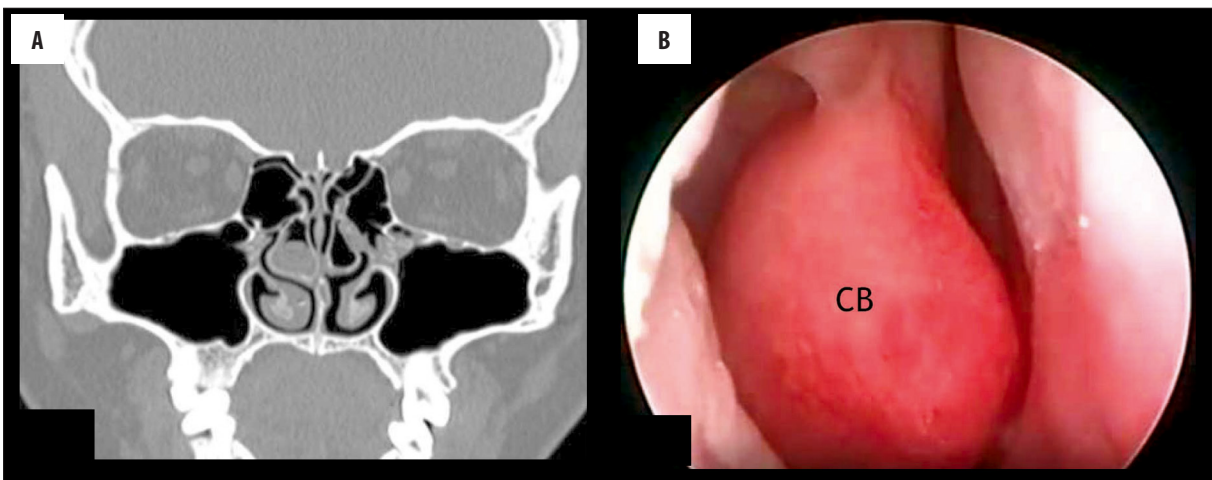
Figure 6. (**A**) MSCT, coronal scans of PNS show bilateral concha bullosa, right-sided (RT) concha bullitis, bilateral paradoxical middle turbinates and right-sided Haller's cells. (**B**) Endoscopic images show right-sided concha bullosa (CB).

compromise the frontal recess, leading to isolated frontal sinusitis. In our study, they comprised 36.7% of all the detected air cells. Importantly, these cells can provide access to the frontal sinus during endoscopy [2]. Haller cells were defined by Mathew et al. in 2013 [14] as ethmoidal air cells that project inferiorly into the floor of the orbit in the region of the maxillary sinus ostium. They reported an incidence of 10% in the general population. In our study, Haller cells were detected in 11.2% of the examined sides, and a half of them compromised the infundibulum.
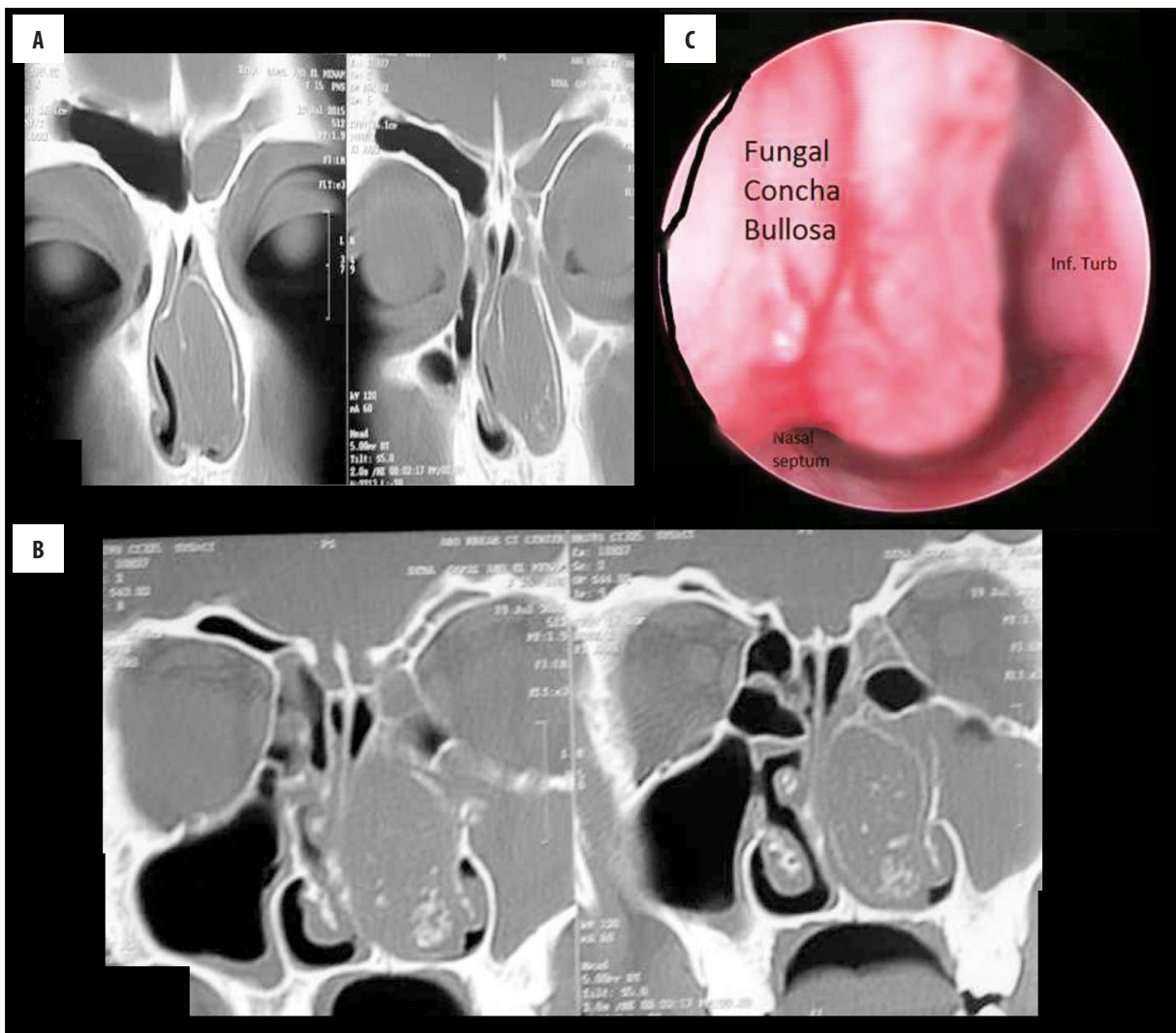
Figure 7. (**A, B**) MSCT, coronal scans of PNS show left-sided concha bullitis containing hyperdense calcific foci, suggesting fungal infection associated with complete obliteration of left-sided maxillary and frontal sinuses that are inflamed; obliterated ipsilateral ostiomeatal complex is also seen. (**C**) Endoscopic images revealed huge left concha bullosa.
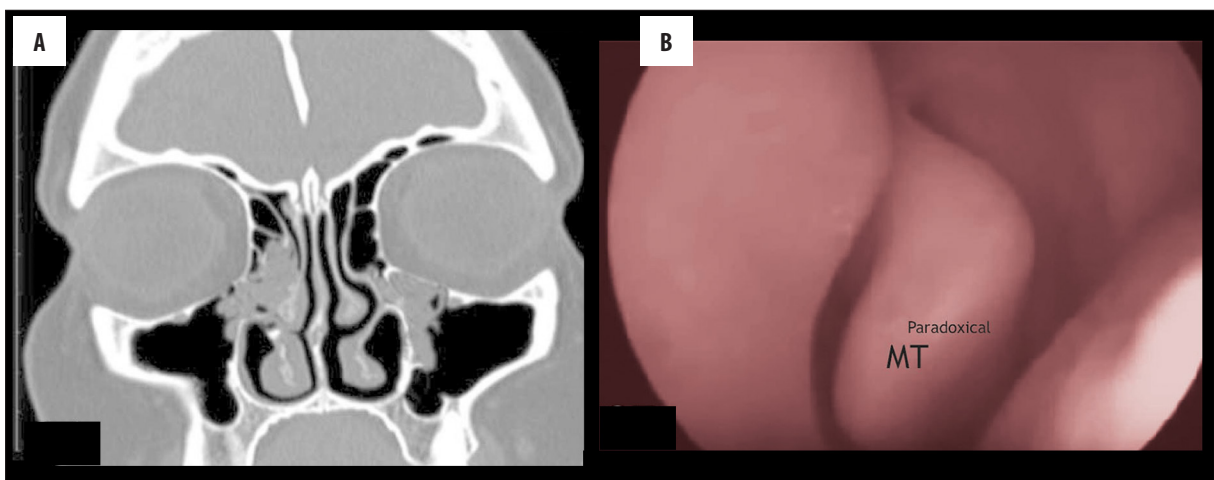

Figure 8. (**A**) MSCT, coronal scans of PNS show left-sided paradoxical middle turbinate and deviated bony nasal septum to the right side associated with bilateral maxillary mucosal thickening of inflamed sinuses and obliterated ostiomeatal complex on both sides. (**B**) Endoscopic image revealed left (LT) paradoxical middle turbinate (MT) and deviated nasal septum.
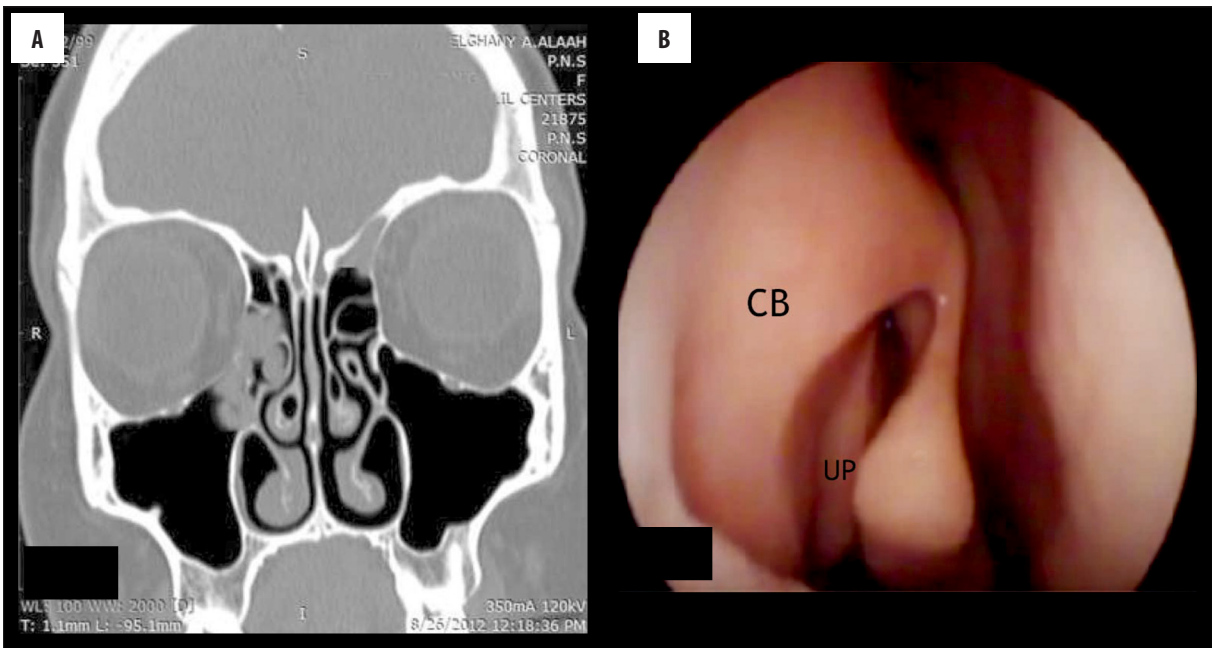
Figure 9. (**A**) MSCT, coronal scans of PNS show medially deviated and pneumatized uncinate processes on both sides that is associated with right ethmoidal sinusitis, obliterated right-sided ostiomeatal complex, and bilateral concha bullosa. (**B**) Endoscopic image shows medially deviated right-sided uncinate process (UP) and concha bullosa (CB).
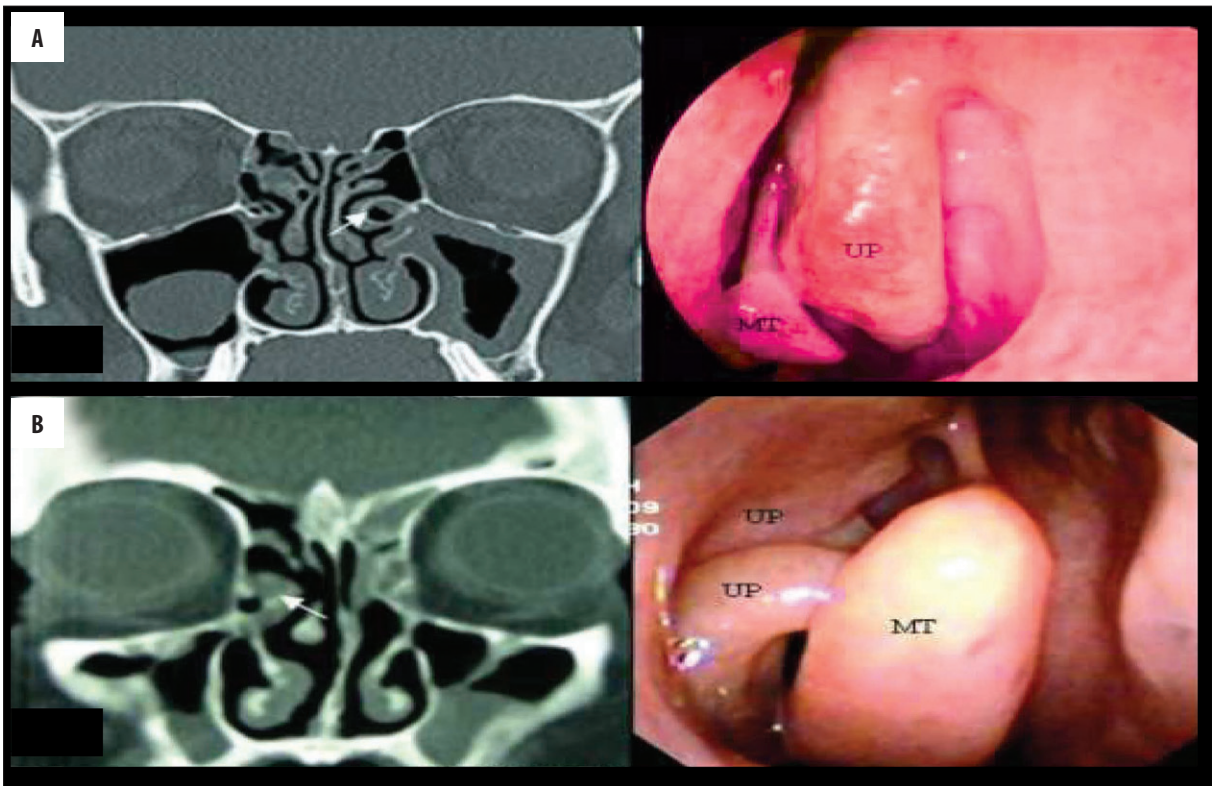

Figure 10. Two different cases. (**A**) MSCT, coronal scan of PNS shows left-sided, hypertrophied, pneumatized uncinate process (arrow) associated with bilateral mucosal maxillary thickening (left circumferentially and right polypoidal). Corresponding endoscopic image revealed hypertrophied left uncinate process. (**B**) MSCT, coronal scan of PNS shows a right-sided, medially bent, obliterated, previously pneumatized uncinate process associated with bilateral basal maxillary sinusitis. Corresponding endoscopic image revealed medial deviation of the uncinate process.
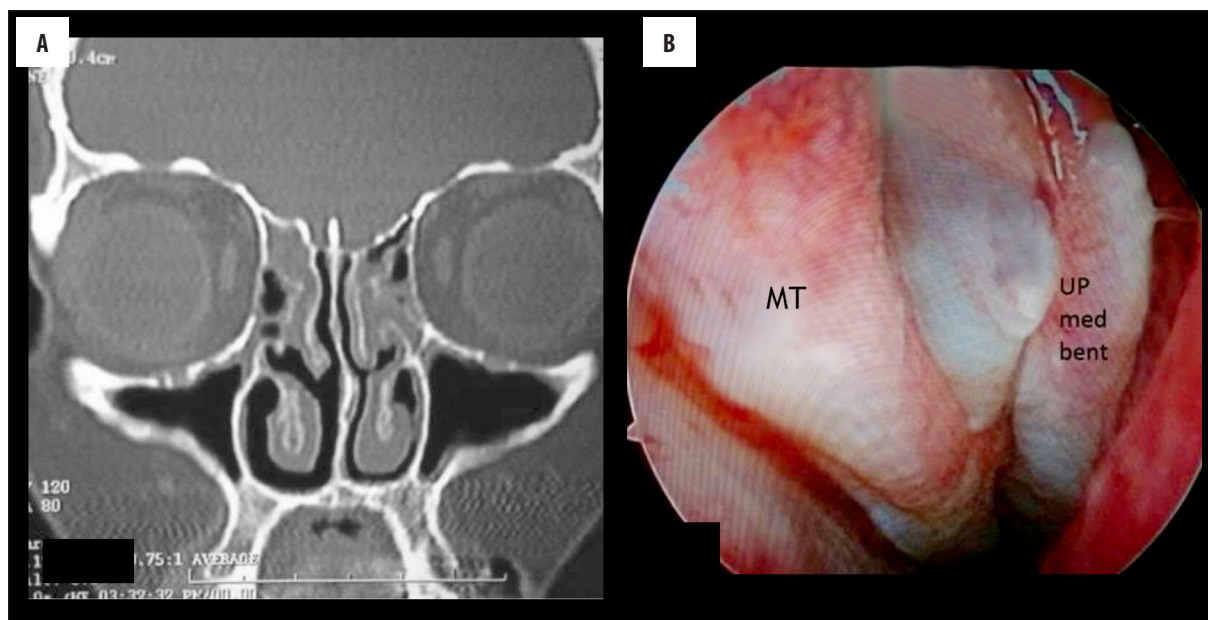
Figure 11. (A) MSCT, coronal scan of PNS shows a left-sided, medially deviated uncinate process associated with bilateral ethmoidal sinusitis. **(B)** Endoscopic image revealed medial deviation of the left uncinate process.

Mathew et al. (2013) [14] found Haller cells in 14% of patients with sinonasal disease; they caused infundibular narrowing in 85.5% of them. Kaygusuz et al. (2014) [9] reported a prevalence of 45%. Katya et al. (2015) [2] consider the presence of these cells as one of the predisposing factors for recurrent maxillary sinusitis (Figures 3–8).

Large ethmoid bulla may compromise the ethmoid infundibulum or middle meatus or may be enlarged and filled with pus [15]. Fadda et al. (2012) [1] reported a high incidence of enlarged ethmoid bulla in 89% of cases. In our study, this finding was detected in 10% of the examined sides.

The uncinate process is a key bony structure in the lateral nasal wall. Together with the adjacent ethmoid bulla, they are defined as the hiatus semilunaris that forms an outlet for a recess – the infundibulum, which is directed anteriorly and inferiorly. The maxillary sinuses open into the posterior aspect of the infundibulum via the ostium [1]. Uncinate process variations were present in 18.1% of the examined sides. When the free margin of uncinate process was enlarged or deformed, it compressed the infundibulum; this was detected in 8.5% of the examined sides. Other, less important variations include pneumatization and hypoplasia [15].

In a large series of 800 patients, Katya et al. (2015) [2] reported that anatomic variations were present in 743 patients, either in isolation or in various combinations; of those, 325 (41%) of cases were endoscopically normal. The authors concluded that anatomic variations can interfere with normal drainage pathways and predispose to sinus disease; this outcome is particularly possible, if the variation occurs at the level of the frontal recess and the ostiomeatal complex. However, anatomic variations can also be found in patients with chronic sinusitis without being the cause of disease [16] (Figures 9–11).

Anatomic variations of paranasal sinus structures may predispose to chronic or recurrent sinusitis and to headaches [17]. However, the relative importance of anatomic variations is still a matter of discussion and variable results have been reported [18].

Conclusions

In patients with chronic or recurrent sinusitis, a thorough inspection of MSCT scans must be performed in order to identify causes of sinus drainage obstruction. Anatomical variations involving the key area of the ostiomeatal complex and frontal recess should be considered.

References:

1. Fadda GL, Rosso S, Aversa S et al: Multiparametric statistical correlations between paranasal sinus anatomic variations and chronic rhinosinusitis. Acta Otorhinolaryngol Ital, 2012; 32(4): 244–51

2. Shpilberg KA, Daniel SC, Doshi AH: CT of anatomic variants of the paranasal sinuses and nasal cavity: Poor correlation with radiologically significant rhinosinusitis but importance in surgical planning. Am J Roentgenol, 2015; 204(6): 1255–60

3. Alkire BC, Bhattacharyya N: An assessment of sinonasal anatomic variants potentially associated with recurrent acute rhinosinusitis. Laryngoscope, 2010; 120: 631–34

4. Al-Abri R, Bhargava D, Al-BassamW et al: Clinically significant anatomical variants of the paranasal sinuses. Oman Med J, 2014; 29(2): 110–13

5. Bhargava D, Bhargava K, Al-Abri A et al: Non allergic rhinitis: Prevalence, clinical profile and knowledge gaps in literature. Oman Med J, 2011; 26(6): 416–20

6. Chen JJ, Chen DJ, Chen CJ: The Lund-Mackay Score for adult head and neck computed tomography. Chinese Journal of Radiology, 2011; 36(4): 203–8

7. Reddy U, Dev B: Anatomical variations of paranasal sinuses on multidetector computed tomography – How does it help FESS surgeons. Indian J Radiol Imaging, 2012; 22(4): 317–24

8. Dalgorf DM, Harvey RJ: Chapter 1: Sinonasal anatomy and function. Am J Rhinol Allergy, 2013; 27(Suppl 1): S3–S6

9. Kaygusuz A, Haksever M, AkdumanD et al: Sinonasal anatomical variations: Their relationship with chronic rhinosinusitis and effect on the severity of disease – a computerized tomography assisted anatomicaland clinical study. Indian J Otolaryngol Head Neck Surg, 2014; 66(3): 260–66

10. Azila A, Irfan M, Rohaizan Y et al: The prevalence of anatomical variations in osteomeatal unit in patients with chronic rhinosinusitis. Med J Malaysia, 2011; 66: 191–94

11. Luo X, Liang C, Xu K et al: [Influence of nasal septal deviation on incidence of bilateral sinusitis.] Lin Chung Er Bi Yan Hou Tou Jing Wai Ke Za Zhi, 2012; 26(17): 777–80 [in Chinese]

12. Yiğit O, Acioğlu E, Cakir ZA et al: Conchabullosa and septal deviation. Eur Arch Otorhinolaryngol, 2010; 267(9): 1397–401

13. Alkire BC, Bhattacharyya N: An assessment of sinonasal anatomic variants potentially associated with recurrent acute rhinosinusitis. Laryngoscope, 2010; 120: 631–34

14. Mathew R, Omami G, Hand A et al: Cone beam CT analysis of Haller cells: Prevalence and clinical significance. Dentomaxillofac Radiol, 2013; 42: 44–55

15. Comer BT, Kincaid NW, Smith NJ et al: Frontal sinus septations predict the presence of supraorbital ethmoid cells. Laryngoscope, 2013; 123: 2090–93

16. Albu S: Novel drug-delivery systems for patients with chronic rhinosinusitis. Drug Des Devel Ther, 2012; 6:125–32

17. Rudmik L, Smith TL: Olfactory improvement after endoscopic sinus surgery. Curr Opin Otolaryngol Head Neck Surg, 2012; 20(1): 29–32

18. Shpilberg KA, Daniel SC, Doshi AH et al: CT of anatomic variants of the paranasal sinuses and nasal cavity: Poor correlation with radiologically significant rhinosinusitis but importance in surgical planning. Am J Roentgenol, 2015; 204(6): 1255–60